2010 International Symposium on Nonlinear Theory and its Applications
NOLTA2010, Krakow, Poland, September 5-8, 2010

Differences between Theoretical and Measured Spectrum in Systems Employing a Spread-Spectrum Clock for EMI Reduction Purposes

Fabio Pareschi[†,§], Gianluca Setti[†,§], Riccardo Rovatti[‡,§] and Giovanni Frattini[¶]

† ENDIF – Engineering Department, University of Ferrara
Via Saragat, 1 – 44100 Ferrara, Italy
‡ DEIS – Department of Electronics, Computer Sciences and Systems, University of Bologna
Viale Risorgimento, 2 – 40136 Bologna
§ Research center "ARCES" – University of Bologna
Via Toffano, 2 – 40125 Bologna
¶ National Semiconductor, Italy
Email: {fabio.pareschi,gianluca.setti}@unife.it, rrovatti@deis.unibo.it, giovanni.frattini@nsc.com

Abstract—Many digital systems employ a *spread spectrum* clock technique for an inherent reduction of the Electro-Magnetic Interference. Spread Spectrum clocking consists in a proper modulation of the system clock, thus reshaping the power density spectrum of all synchronized digital signal. The aim of this paper is to show that, depending on the specific setting, very large differences between the theoretically computed power density spectrum and the measured one arise. This is an important issue to take into consideration when a Spread Spectrum system is optimized for EMI reduction.

1. Introduction

The reduction of the Electro-Magnetic Interference (EMI) in electronic system is an inherent problem in all modern digital equipment. In fact digital signals, due to their sharp edges and their synchronization with a periodic clock waveform, are preeminent sources of interference, since they give arise to a large amount of interfering power in a narrow-band frequency range.

This point of view is coherent with many regulations [1, 2] which link compliance, or Electro-Magnetic Compatibility (EMC), with the ability to constrain the interfering power density spectrum (PDS) within a prescribed mask.

The reason why EMI are related to the shape of the interfering signal PDS, in particular to its peak value, is that in the coupling process between EMI sources and third-party nearby circuits (EMI victims), these latter can be usually modeled as a number of narrowband filters, i.e. a victim is sensitive only in a few frequency ranges. The worst case scenario is when the PDS of an interfering signal is composed by few components with a high power level (as for a synchronous digital system) and the largest of them is exactly located in one of the victim sensitivity frequency ranges. In this case all its power is transferred to the victim, potentially yielding to its complete failure.

It is worth noticing that in addition to common solutions to increase the EMC which are based on *a-posteriori* methodologies (such as the adoption of filters, shielded cables and filtered connectors) which aim at reducing the coupling between EMI sources and EMI victims, some *design-time* solutions, usually known as *spread spectrum* clocking techniques, can be adopted.

Referring to [3], spread spectrum clocking is defined as *"a technique to reduce the emission from all signals synchronized with a clock"* and, roughly speaking, consists of introducing a controlled jitter in the reference clock, thus avoiding a perfect periodicity of all the synchronized signals. This gives rise to additional components in the PDS, while, at the same time, it lowers the power of the already present ones, with a positive effect in EMI reduction.

In this paper we consider the differences between the theoretical PDS of a spread spectrum system and the spectrum measured according to EMC regulations. This is particularly import since, despite the fact that most common way to design a spread spectrum system is to reshape the theoretical PDS [4, 5], regulations require that measurements are taken in a prescribed setting with an EMI receiver, (which is an analog Spectrum Analyzer): we can show that the theoretical spectrum and the measured one match only for particular cases.

The organization of the paper can be summarized as follows. The aim of the Section 2 is to provide a brief theoretical background. Here, we first introduce the working principle of the analog spectrum analyzer. Then, we consider a Spread Spectrum clock system based on the Frequency Modulation (FM) of the clock with a sinusoidal waveform as driving signal. Despite the fact that this approach is not commonly used in real systems, where a clock FM with a triangular waveform [6, 7], a more complex and patented periodic waveform [3] or a Pulse-Amplitude Modulated (PAM) waveform [8, 9] is used as driving signal, the sinusoidal case is interesting since its theoretical PDS can be expressed in a simple, closed form. In Section 3 this PDS is compared with the measured spectrum, and despite being the latter very complex to compute, we will be able to easily explain why and under which circumstances differences exist between the two. Finally in Section 4 we draw the conclusion.

2. Mathematical Background

2.1. Working Principle of a Spectrum Analyzer

An analog Spectrum Analyzer is based on a superheterodyne receiver as schematized in Figure 1(a). The input sig-

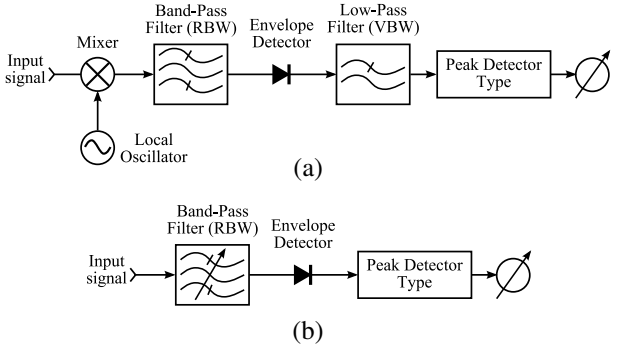

Figure 1: (a) Actual and (b) simplified block diagram of an analog Spectrum Analyzer.

nal is mixed with a pure tone generated by a local oscillator to shift it in a lower frequency range and then filtered by narrow band-pass filter (whose bandwidth is called Resolution BandWidth, RBW). The resulting output signal is then demodulated by an envelope detector, low-pass filtered (the VBW) and its power level is measured by a peak detector. Note that this must be distinguished from the digital spectrum analyzer, or *Digital Signal Analyzer*, which is based on the real-time Fourier transform of the sampled input signal.

By changing the local oscillator frequency, it is possible to tune a different frequency band on the RBW filter, so that to measure the spectrum of the input signal, it is enough to tune the system to all the frequency of interest.

The EMI regulations allows the use of both the *quasi-peak detector* and the *positive peak detector*. For the sake of simplicity, we consider here only the latter, which estimate the power of the tuned signal as the power of a pure sinusoidal tone whose amplitude is equal to the maximum amplitude detected while the system is tuned to a given frequency.

Note that the same measurement results can be achieved by a system like the one in Figure 1(b), where the signal is tuned by properly setting the central frequency of the RBW filter. The VBW filter is not considered since under the common assumption of VBW > RBW its effect can be neglected. This will be more clear at the end of Section 3. In the following, we will always refer to this simplified diagram.

A detailed survey on this instrument can be found in [10], where the RBW filter is assumed as a four-pole system, with nearly-Gaussian transfer function

$$|H(f; f_0, \mathrm{RBW})|^2 = \frac{1}{\left(1 + \left(\frac{f - f_0}{\nu_0\,\mathrm{RBW}}\right)^2\right)^4} \qquad (1)$$

where f_0 is the center frequency and $\nu_0 = \dfrac{1}{2\sqrt{2^{1/4} - 1}}$ and the RBW is defined as the -3 dB filter bandwidth.

2.2. Sinusoidal FM

Let us consider here an FM clock signal which, referring to the first harmonic only, can be written as

$$s(t) = A\cos\left(2\pi f_c t + 2\pi Df \int_{-\infty}^{t} \xi(\tau)d\tau\right)$$

where $-1 < \xi(t) < 1$ is the normalized driving signal, and Df the frequency deviation. It is worth stressing that considering only the fundamental tone of a timing signal is a standard practice for EMI measurement purposes, since it is the harmonic giving rise to highest peaks in the spectrum, and which is therefore responsible for generating the most severe EMI components.

When using a sinusoidal waveform as driving signal, i.e. $\xi(t) = \cos(2\pi f_m t)$, we get $s(t) = A\cos(2\pi f_c t + m\sin(2\pi f_m t))$, with $m = Df/f_m$ is known as *modulation index*.

The PDS $S(f)$ of $s(t)$ is a discrete spectrum with components at all frequencies $f_c \pm k f_m$, $\forall k \in \mathbb{N}$, and can be written using the first kind Bessel Function [11]

$$S(f) = \frac{A^2}{2}\sum_{k=-\infty}^{\infty} J_k^2(m)\,\delta\left(f - f_c - \frac{k}{m}Df\right) \qquad (2)$$

3. Comparison between Theoretical Spectrum and Measured One

The theoretical spectrum of a sinusoidal FM measured by means of a band-pass filter is given by the convolution of (2) with the filter transfer function, which is given by (1), so that we get

$$S^{(th)}(f) = \frac{A^2}{2}\sum_{k=-\infty}^{\infty} J_k^2(m)\left|H\left(f; f_c + \frac{k}{m}Df, \mathrm{RBW}\right)\right|^2 \qquad (3)$$

The spectra achieved for $f_c = 1$ MHz, $Df = 50$ KHz, RBW = 3 KHz and different values of m are shown in Figures 2(a), 2(b) and 2(c). In all Figures the 0 dBc reference level is the power level of the first harmonic of the unmodulated clock, i.e. is $A^2/2$.

Figures 2(d), 2(e) and 2(f) show, for the same cases, the spectrum measured with an HP8563E Spectrum Analyzer. Similarly, the 0 dBm reference level is the power level of the first harmonic of unmodulated clock.

By comparing the two sets of Figures, some remarks can be made.

- In the case when m is low (Figures 2(a) and 2(d), where $m = 3$) the match between the spectrum expected according to (3) and the measured one is almost perfect.

- When m assumes intermediate values (as in Figures 2(b) and 2(e), where $m = 25$) despite a good matching between the shape of the expected and the measured spectrum, the measured one has a much higher level then the expected one. In this example, the difference is approximately 5 dB.

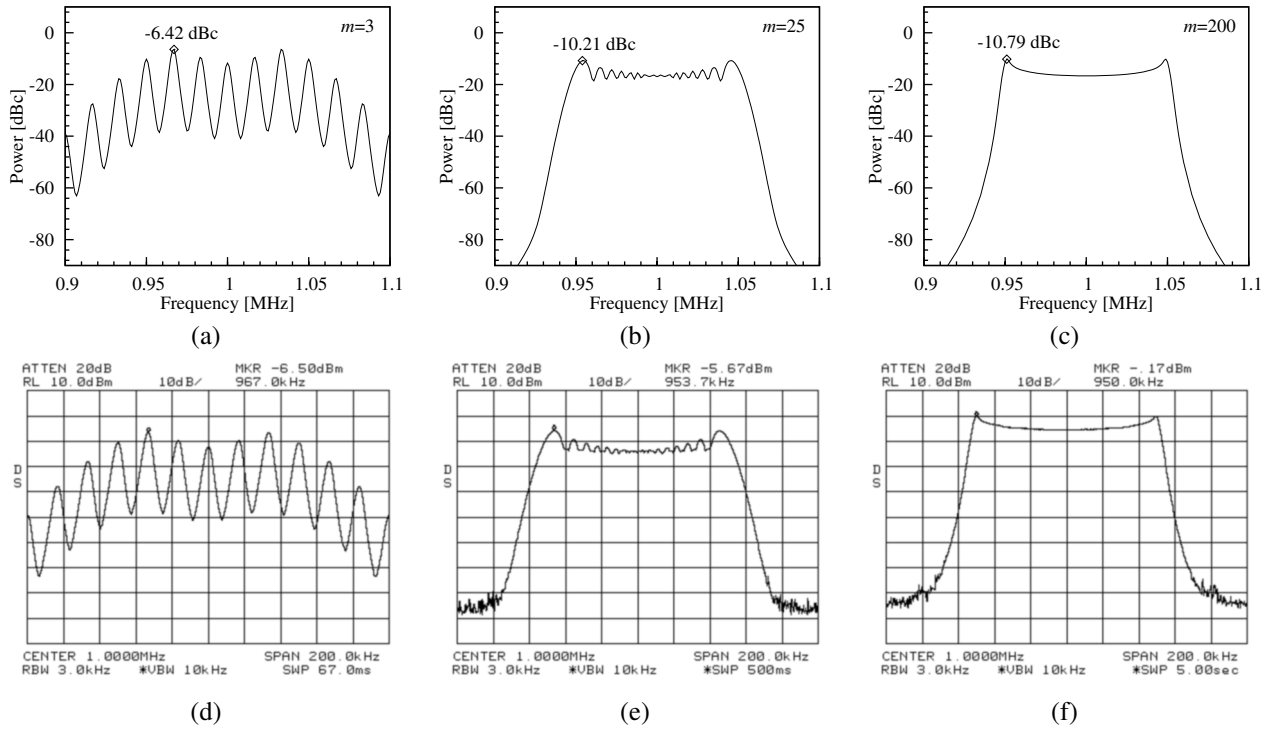

Figure 2: Comparison between the power spectrum expected from Equation (3) and the one measured from an HP8563E Spectrum Analyzer. (a) Expected spectrum for $m = 3$; (b) expected spectrum for $m = 25$; (c) expected spectrum for $m = 200$; (d) measured spectrum for $m = 3$; (e) measured spectrum for $m = 25$; and (f) measured spectrum for $m = 200$. In all cases, it is $f_c = 1$ MHz, $Df = 50$ KHz, RBW = 3 KHz.

- For very large values of m (Figures 2(c) and 2(f), where $m = 200$) the difference between the expected and the measured spectrum is increasing (about 10 dB in this case). Furthermore, the shapes of the two spectra do not match anymore, as in the measured one a saturation effect seems to arise. Note also that the peak level of the measured spectrum is almost equal to the unmodultaed signal power.

Even if, for the sake of simplicity, we have considered the sinosoidal case, comments similar to those above can be made for any modulating signal, including all those which are used in practical application (triangular [6, 7], patented [3] and PAM [8, 9]). These observations have a serious impact on the design of a spread spectrum clocking system for EMI reduction.

In fact, to the best of our knowledge, the way which is almost always adopted to design a spread spectrum system is to optimize its performance according to the *theoretical PDS*, i.e. according to the spectrum one could expect from Equation (3). In this case, as it is clear from the above example, the highest EMI reduction is given when m has intermediate or large values, with more then 10 dB reduction in the peak level in the power spectrum with respect to the unmodulated case. Like in the case of the example, most of the actual spread spectrum systems are designed [3, 6, 8] to operate with reasonably very large values of m, as the performance of a spread spectrum system is optimized for $m \to \infty$.

What we want to show with the above example is that, as m increases, the differences between the expected and the measured spectrum also increase. More important, when m assumes very large values (as in the case of Figure 2(f)), the EMI reduction with respect to the unmodulated case may become negligible, i.e. cases exist where a spread spectrum system would give *no advantages* in terms of EMI reduction.

Despite the fact that a formal mathematical explanation of this effect would be extremely complex, we can give a simple, intuitive one. It is known that the positive peak detector may overestimate the power of the filtered signal. It is common to say that it gives results higher than the quasi peak detector, which gives results higher than the average detector. Note however that neither the quasi peak nor the average detector are usually present in a standard spectrum analyzer. The overestimation of the positive peak detector depends on the features of the analyzed signal. In the considered case, it is clear that, the higher is m, the higher the overestimation.

Let us consider a *slow* sinusoidal modulation, i.e. the case where m is very high or, equivalently, f_m is very low. Let us also refer to the block diagram of Figure 1(b). We can model the system as slowly changing its *instantaneous frequency* from $f_c - Df$ to $f_c + Df$. When the time required for sweeping from $f_0 - \text{RBW}/2$ to $f_0 + \text{RBW}/2$ (i.e. the time to completely cross the RBW filter bandwidth) is long enough, the Spectrum Analyzer sees the signal as virtually "unmodulated" and the amplitude memorized by the peak detector is almost equal to the amplitude memorized in the

actual non-modulated case.

From a mathematical point of view, we can consider the simple case in which $f_0 = f_c$. Let us also consider that the RBW filter is an ideal rectangular band-pass filter. In the theoretical spectrum, only components with frequency $f_c - \text{RBW}/2 \leq f \leq f_c + \text{RBW}/2$ will contribute to the power at f_c

$$S^{(th)}(f_c) = \frac{A^2}{2} \sum_k J_k^2(m), \quad |k| \leq \frac{1}{2}\, m\, \frac{\text{RBW}}{Df} \tag{4}$$

When using the model of Figure 1(b), it is easy to understand that the signal at the input of the peak detector can be computed as the absolute value of the *complex envelope* $\tilde{s}(t)$ of the signal $s(t)$ being filtered by the base-band equivalent of the RBW filter, which is a low-pass filter with bandwidth RBW /2. Note that it is now clear that the condition for neglecting the VBW filter is VBW > RBW /2, which is usually satisfied.

Since the input signal can be written as

$$s(t) = \text{Re}\left(A e^{j2\pi f_c t + jm\sin(2\pi f_m t)}\right)$$

its complex envelope is [11]

$$\tilde{s}(t) = A e^{j\sin(2k\pi f_m t)} = \sum_{k=-\infty}^{\infty} J_k(m)\, e^{j2\pi f_m t}$$

Under the assumption of a rectangular low-pass filter with bandwidth RBW /2, the filtered complex envelope $\tilde{s}_H(t)$ is obtained by considering the only few components

$$\tilde{s}_H(t) = A \sum_k J_k(m)\, e^{j2k\pi f_m t}, \quad |k| \leq \frac{1}{2}\, m\, \frac{\text{RBW}}{Df}$$

The signal power is estimate by the positive peak detector as $\frac{1}{2}\left(\max_t |\tilde{s}_H(t)|\right)^2$. Note that independently on the number of considered components, $|\tilde{s}_H(t)|$ is periodic with a maximum for $t = \frac{k}{f_m} \pm \frac{1}{4 f_m}$; the power measured in f_c by the positive peak detector is

$$S^{(meas)}(f_c) = \frac{A^2}{2} \left| \sum_k j^k\, J_k(m) \right|^2, \quad |k| \leq \frac{1}{2}\, m\, \frac{\text{RBW}}{Df} \tag{5}$$

By comparing Equation (4) with Equation (5) we can determine when the measured spectrum differs from the theoretical PDS. Despite the fact that the two above expression are very difficult to handle with, it is possible to see that one always have $S^{(th)}(f_c) \leq S^{(meas)}(f_c)$. Furthermore, the only condition for which we can ensure a matching between the two spectra is $\frac{1}{2}\, m\, \frac{\text{RBW}}{Df} < 1$. In this case, both the sums of Equation (4) and Equation (5) result in

$$S^{(th)}(f_c) = S^{(meas)}(f_c) = \frac{A^2 J_0^2(m)}{2}$$

In conclusion, based on what computed for the power spectrum at frequency f_c, we can say that in a fast modulation, more precisely when $m < 2\frac{Df}{\text{RBW}}$ (which means $f_m > \text{RBW}/2$) we can be sure that the measured spectrum matches the theoretical PDS. On the contrary, when $m > 2\frac{Df}{\text{RBW}}$ we can expect a power level of the measured spectrum higher than the one computed through the theoretical PDS.

4. Conclusion

In this paper we have compared the theoretical PDS of a sinusoidal Frequency Modulation with the spectrum achieved by a measurement with a Spectrum Analyzer. By means of a very simple modeling of this instrument, we have concluded that the two spectra match only when the modulation index $m < 2\frac{Df}{\text{RBW}}$. Otherwise, the measured power level is higher than the expected one from the theoretical PDS. This has important consequences in spread spectrum systems based on the frequency modulation of the clock, since the EMI reduction measured according to EMC regulations may be much smaller than the expected one when m is too large.

References

[1] National Archives and Records Administration's Office, Code of Federal Regulations. 47 (47CFR), part 15, subpart B: "Unintentional Radiators".

[2] Official Journal of the European Communities, "Council Directive on the approximation of the laws of the Member States relating to electromagnetic compatibility" (89/336/EEC), No. L139/19, May 23, 1989.

[3] K.B. Hardin, J.T. Fessler, D.R. Bush, "Spread spectrum clock generation for the reduction of radiated emission", in *Proc. Int. Symp. Electromagnetic Compatibility*, pp. 227-231. Aug. 1994.

[4] A. Stankovic, H. Lev-Hari, "Randomized Modulation in Power Electronic Converters", *Proceedings of the IEEE*, Vol. 90, No. 5, pp. 782-799. May 2002.

[5] F. Lin, D. Y. Chen, "Reduction of Power Supply EMI Emission by Switching Frequency Modulation", in *IEEE Trans. on Power Electronics*, vol. 9, no. 1, pp. 132–137. Jan 1994.

[6] Serial ATA International Organization, "Serial ATA Revision 2.6", Feb. 2007.

[7] -, "LM 5088 - Wide Input Range Non-Synchronous Buck Controller". Datasheet from National Semiconductor. June 2009.

[8] F. Pareschi, G. Setti, and R. Rovatti, "A 3 GHz Spread Spectrum Clock Generator for SATA Applications using Chaotic Pam Modulation", in *Proc. IEEE Custom Integrated Circuits Conference CICC '08*, pp. 451–454. Sept. 2008.

[9] -, "LTC6908 - Dual Output Oscillator with Spread Spectrum Modulation". Datasheet from Linear Technology. 2008.

[10] -, "Spectrum Analysis Basics", Agilent Application Note 150. June 2006.

[11] H. S. Black, *Modulation Theory*, Van Nostrand, 1953.